Journal of Air Pollution and Health (Autumn 2022); 7(4): 375-398

Original Article

Available online at http://japh.tums.ac.ir

Investigating the mechanism of dust transferring from Iraq to the north of Alborz mountains in Iran

Sara Karami[1], *Zahra Ghassabi*[2,*], *Parviz Rezazadeh*[3]

[1] Air Pollution and Dust Research Group, Atmospheric Science and Meteorological Research Center (ASMERC), Tehran, Iran
[2] Atmospheric Hazard Forecast Group, Atmospheric Science and Meteorological Research Center (ASMERC), Tehran, Iran
[3] Meteorological Consultant, Iran Meteorological Organization (IRIMO), Tehran, Iran

ARTICLE INFORMATION

Article Chronology:
Received 11 September 2022
Revised 26 October 2022
Accepted 10 November 2022
Published 30 December 2022

Keywords:
Dust storm; Topography; Cold front; Ascending motions; Weather research and forecasting model coupled with chemistry (WRF-Chem)

CORRESPONDING AUTHOR:

z.ghassabi@gmail.com
Tel : (+98 21) 44787651
Fax : (+98 21) 44787670

ABSTRACT

Introduction: Recently, due to climate change, the number and intensity of dust sources are increasing, which leads to the occurrence of dust storms. Atmospheric patterns governing the region, topography and surface features are effective on transportation and dispersion of dust particles.

Materials and methods: In this study, a severe dust phenomenon on the 3th and 4th March, 2022, was investigated. The dust was emitted from the east of Iraq and passed through the Zagros and Alborz mountain ranges toward the Caspian sea. Meteorological data of the country, satellite data, ERA5 reanalysis data and HYSPLIT and output from the Weather Research and Forecasting Model coupled with Chemistry (WRF-Chem) were used.

Results: Aerosol Optical Depth (AOD) anomaly compared to the long-term indicated that the intense transport of dust particles from eastern Iraq and reaching the Caspian Sea is not a common phenomenon. Synoptic analysis showed that the dust particles in the source area ascended to the mid-levels of the atmosphere and a large part of the particles passed through the Zagros Mountains. Then, the dust entered the Caspian Sea by passing through the Manjil valley. The vertical profile of WRF-Chem model output showed the ascent of dust particles up to 600 hPa near the dust source and its passage over mountainous areas.

Conclusion: The main factors in the formation of this unusual dust phenomenon are: severe two-year drought in the Middle East, reduction of vegetation and cold front of the dynamic low-pressure located in the east of the Black Sea, east of Turkey and northern Iraq moving eastward to the Caspian sea in the following hours.

Introduction

The occurrence of dust storms every year in many regions of the world causes a lot of financial and human losses. Dust storms cause severe heart and respiratory diseases [1-3]. An increase in road accidents and flight cancellations due to severely reduced visibility are among the financial losses caused by dust [4, 5]. Dust also causes severe damage to the industry and energy sectors, including water and electricity cuts [6], reducing the power of wind turbines and solar cells [7]. The settling of dust particles on industrial equipment also causes destruction and reduction of their power [8].

In recent years, due to climate change, the

Please cite this article as: Karami S, Ghassabi Z, Rezazadeh P. Investigating the mechanism of dust transferring from Iraq to the north of Alborz mountains in Iran. Journal of Air Pollution and Health. 2022;7(4): 375-398.

number of dust sources and the intensity of their activity are increasing in different regions of the world [9, 10]. Their activity causes dust storms. Atmospheric patterns governing the region are effective on the intensity of dust sources activity and also on how dust particles are transported and dispersed [11]. Many studies have been conducted in relation to the investigation of synoptic conditions affecting the formation of dust storms [12-14]. The transport path of dust particles is affected by topography and surface effects [15]. Many researchers conducted a study on the effect of topography on the vertical transport of dust particles in the atmosphere, they concluded that topography increases the probability of large dust particles (diameter 60 μm) reaching high altitudes, which is caused by the upslope flow and the turbulence behind the mountain.

Iraq, located in the Middle East, is one of the regions that has a large number of dust sources; their activity causes severe dust storms in this country and dust transmission to other neighborhood countries [18, 19]. The blowing of north and north-west winds over Iraq, which called "Shamal wind", especially in the summer season, causes dust to be transferred from Iraq to the west and south-west of Iran, Kuwait, northern Arabia and Persian Gulf [20-22]. Insufficient moisture in the atmosphere as well as the surface, strong winds with cold fronts, especially in spring and winter, also cause dust emission from the Iraq and its transfer to neighboring areas [23-24]. The Zagros mountain range, which stretches from the north-west to the south of Iran, plays an important role in the formation of the Shamal wind over the country of Iraq due to the creation of mountain high pressure. It often prevents the entry of some of the dust particles emitted from Iraq to the central regions of Iran [25, 26]. It should be noted that in some cases, dust particles have entered the central regions of Iran due to extreme instability and penetration of particles into the atmospheric mid-layers [27]. Also, in many cases, the Alborz mountain range in the north of Iran prevents the transfer of advective dust from neighboring countries or dust from the central regions of the country to the southern shores of the Caspian sea [28]. In a study to investigate the effect of the Zagros mountain range on dust transport from Iraq to Iran, three numerical experiments were conducted using the WRF-Chem model [29]. One experiment in natural state, one in the state that the topography height is reduced to 1000 m and the other with complete removal of topography. In the natural state, dust concentration increased in the west of Zagros mountain range. The removed topographic height causes the movement of dust towards the east of the mountain and the reduction of dust concentration in the western slope of the mountain range.In a study to investigate the effect of the Zagros mountain range on dust transport from Iraq to Iran, three numerical experiments were conducted using the Weather Research and Forecasting model coupled with Chemistry (WRF-Chem) model [29]. One experiment in natural state, one in the state that the topography height is reduced to 1000 m and the other with complete removal of topography. In the natural state, dust concentration increased in the west of Zagros mountain range. The removed topographic height causes the movement of dust towards the east of the mountain and the reduction of dust concentration in the western slope of the mountain range.

In this study, a case of severe dust phenomenon, during which dust particles were emitted from different dust sources in Iraq and Syria, southwest Iran and central regions of the country, is investigated and simulated. Of course, the main focus of the study is on the dust transfer from the east of Iraq near the border of Iran to the Caspian Sea. The noteworthy point in this case is the transfer of dust from the dust source to the Caspian Sea by passing over the Zagros mountain range and through the Alborz Mountains. The reminder of this paper is organized as follows: Section 2 introduces the study area, Materials and Methods. Section 3 presents the results of observational and analysis data, satellite data and products, synoptic analysis and the trajectory and dispersion models of the Hybrid Single-Particle Lagrangian Integrated Trajectory (HYSPLIT)

and the Weather Research and Forecasting model coupled with Chemistry (WRF-Chem) model; and Section 4 summarizes the findings and conclusions.

Materials and methods

In this study, a severe dust on March 3th and 4th, 2022, during which the dust was emitted from the border areas of Iran and Iraq and was transported to the Caspian sea by passing through the Zagros and Alborz mountain ranges, has been investigated and simulated. In order to investigate the areas affected by dust, first the present weather code and the visibility of the synoptic stations of Iran were studied. The temporal and spatial pattern of dust in the region was investigated using Dust RGB images of Meteosat Second Generation (MSG) satellite, which is available with an hourly interval. Afterward, the mean Aerosol Optical Depth (AOD) from the Moderate Resolution Imaging Spectroradiometer (MODIS)/Aqua with a spatial resolution of 1° on March during 2003-2022 (20 years) as well as its anomaly on March 3 and 4, 2022 compared to the average values were displayed. To investigate the change in the activity of the dust source from which the emitted particles have been transported to the south of the Caspian Sea (red rectangle in Fig. 1) and some affecting factors over time, the mean AOD, Enhanced Vegetation Index (EVI) index and the cumulative precipitation of March timeseries was studied over 2003-2022.

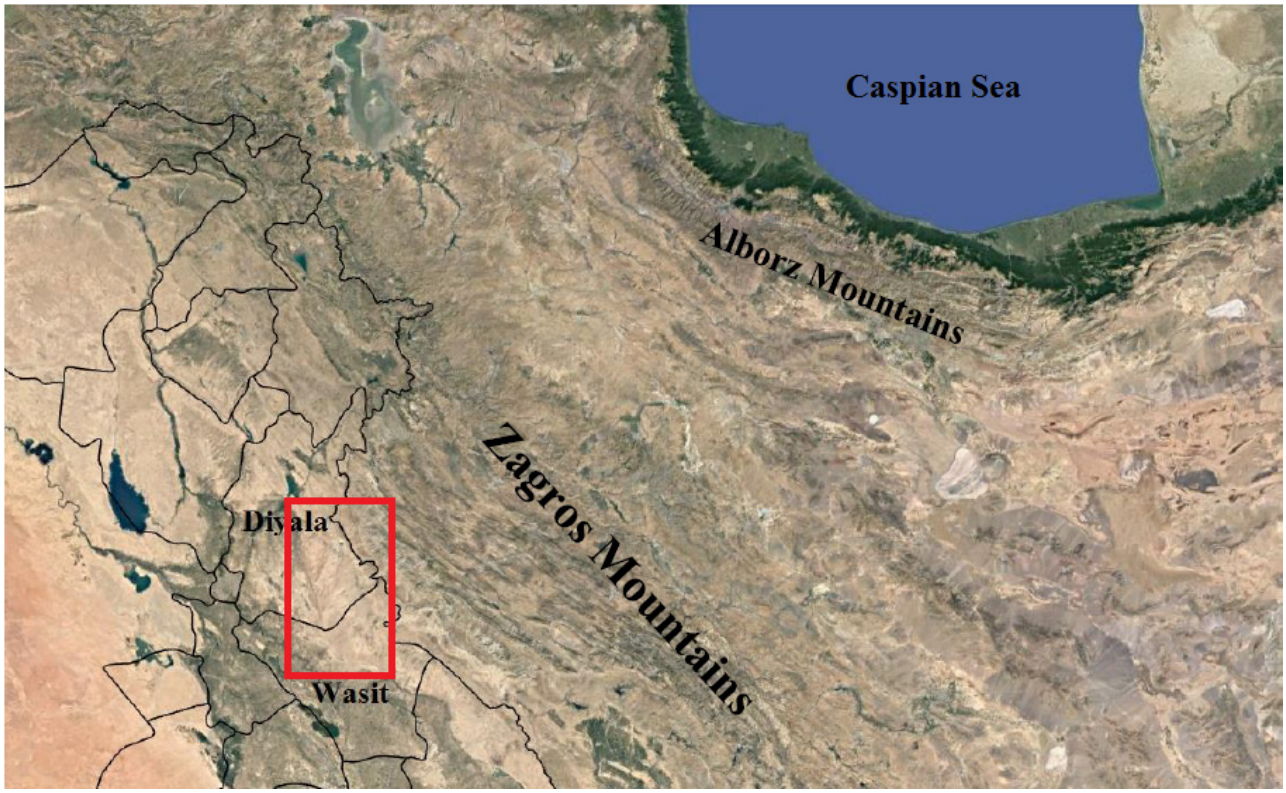

Fig. 1.Topography of the study area. The red rectangle shows the desired dust source

country to the southern shores of the Caspian sea [28]. In a study to investigate the effect of the Zagros mountain range on dust transport from Iraq to Iran, three numerical experiments were conducted using the WRF-Chem model [29]. One experiment in natural state, one in the state that the topography height is reduced to 1000 m and the other with comos mountain range and through the Alborz Mountains. The reminder of this paper is organized as follows: Section 2 introduces the study area, Materials and Methods. Section 3 presents the results of observational and analysis data, satellite data and products, synoptic analysis and the trajectory and dispersion models of the Hybrid Single-Particle Lagrangian Integrated Trajectory (HYSPLIT).

$$EVI = G \times \frac{(NIR - Red)}{(NIR + C1 \times Red - C2 \times Blue + L)} \quad (1)$$

Where: NIR/Red/Blue are surface reflections corrected by the atmosphere (Rayleigh absorption and ozone) in the range of blue, red and infrared wavelengths.

L is the canopy background adjuster, which deals with the nonlinear and differential transmission of red and NIR radiation through the canopy. C1 and C2 are the coefficients of the resistance part of aerosols that use the blue band to correct the effects of aerosols in the red band. The coefficients used in the MODIS-EVI algorithm are: L=1, C1=6, C2=7.5, and G=2.5 (increase coefficient).

Global Precipitation Measurement (GPM) daily cumulative rainfall data was used for precipitation analysis. This dataset includes level 3 data and the result of The Integrated Multi-satellitE Retrievals for GPM (IMERG) algorithm. In the main algorithm of IMERG, the estimation of precipitation is done using the various precipitation-relevant satellite passive microwave (PMW) sensors. Then gridded, intercalibrated to the GPM Combined Ku Radar-Radiometer Algorithm (CORRA) product, and merged into half-hourly 0.1°×0.1° (roughly 10 ×10 km) fields.

Regarding to the prominent role of atmospheric patterns in the dust emission and transfer to other regions, the maps of mean sea level pressure (MSL); wind speed, temperature, geopotential height (GPH), Omega and LI at 850 hPa, GPH of 500 hPa as well as wind speed at 700 hPa and 300 hPa are plotted using gdas/FNL data with spatial resolution of 0.25°.Considering that dust transport over high mountains is a rare phenomenon in the study area, anomaly patterns of some parameters were studied, including: MSL, GPH, omega and wind speed at 850 hPa and GPH of 500 hPa.

The dust particle transport investigated by the HYSPLIT trajectory and dispersion model which has been implemented forward from the dust source at an initial height of 500 m using GFS data with 0.25° horizontal resolution.

The simulation of this dust storm has been done using the WRF-Chem model with the Air Force Weather Agency (AFWA) emission scheme. The AFWA scheme is a modified version of the dust emission scheme based on particle saltation [30], and considers dust emission as a two-part process in which large particle saltation is induced by wind formation and lead to emission. Fine particles are bombarded and decomposed. The equations of the AFWA schema are obtained in terms of frictional velocity and include the statistical threshold frictional velocity required for particles, horizontal saltation flux, vertical flux of bulk dust, size distribution of emitted dust particles and dust flux according to particle size. Various data is used to calculate dust flux from the surface. Data related to land surface and soil texture are available in the model database, and variable quantities such as wind velocity and soil moisture are calculated in the meteorological section of the model at each time step. This model is implemented on a horizontal resolution of 21 km and 45 vertical levels (Fig. 2). Some schemas used in the implementation of the model are shown in the Table1. gdas/FNL data with spatial resolution of 0.25° is used for initial and boundary condition of WRF-Chem model.

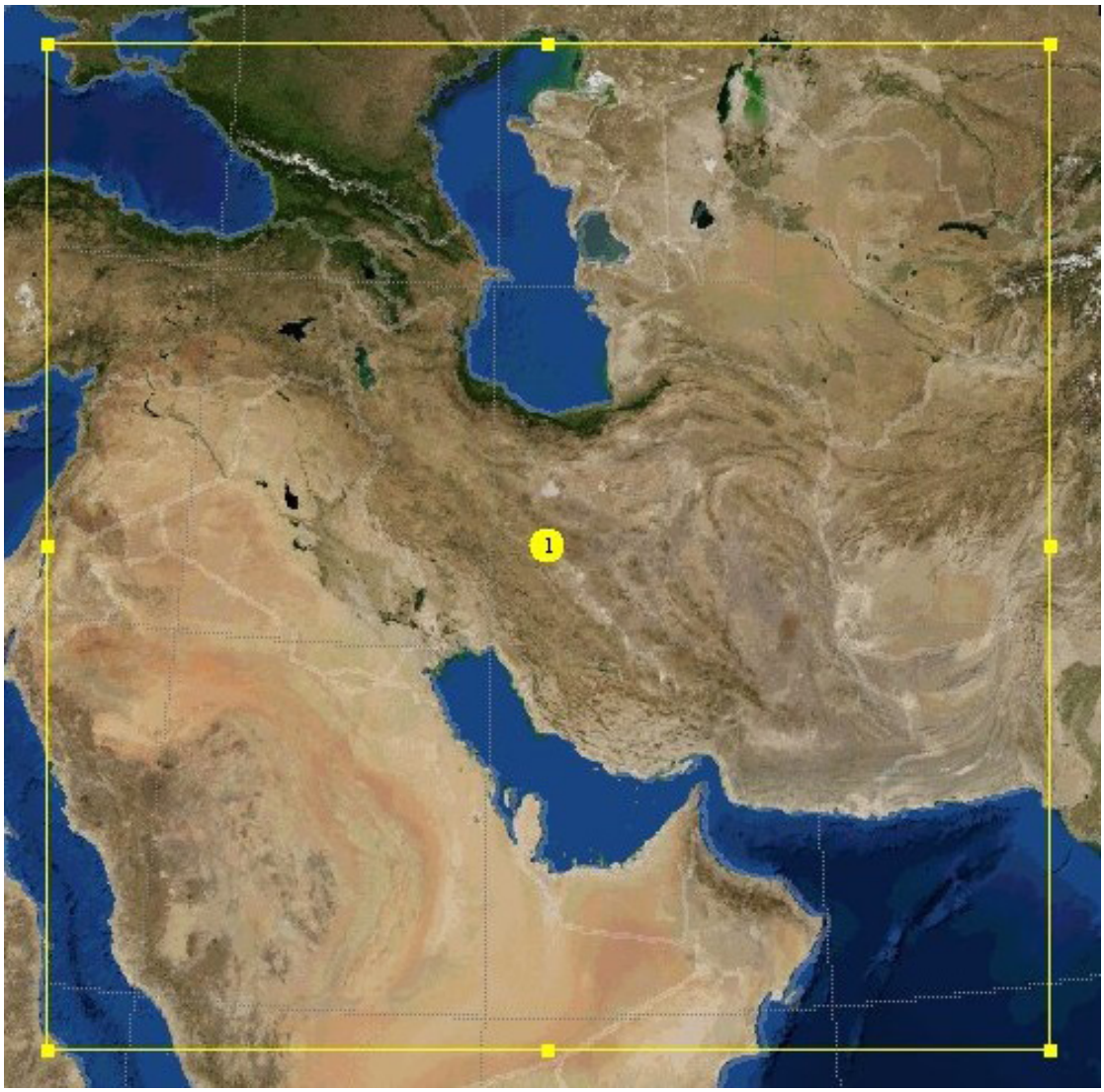

Fig. 2. Model simulation domain

Table 1. Some schematics used in the implementation of the WRF-Chem model

Microphysics	WRF single-moment 5-class scheme
Long wave radiation	RRTM scheme [31]
Short wave radiation	Goddard shortwave [32]
Surface physics	Noah Land Surface Model [33]
Planetary boundary layer	Yonsei University scheme [34, 35]
Cumulus	Grell 3D [36]

Results and discussion

Observation

Fig. 3 shows the horizontal visibility at all the synoptic stations in Iran that have reported dust at 12 UTC on March 4, 2022. Dust reported in a large part of Iran, however the maximum decrease in horizontal visibility was in the western part of the country, so that the horizontal visibility reached less than 1000 m in most of stations in western Iran. The dust phenomenon surrounded the west of Iran to the southern shores of the Caspian Sea, and the horizontal visibility reached less than 5 km.

Satellite products and data

Many studies have been used Dust RGB products to detect dust masses [37, 39]. Dust RGB images of MSG satellite on March 4, 2022 are shown in Fig. 4. In these pictures, the dust mass is shown with pink color. At 03:00 UTC, dust can be seen in the east of Iraq and the border areas with Iran. At 06:00 UTC, the dust mass entered the western regions of Iran and surrounded the north of Iran and the Caspian Sea. At 09:00 UTC, dust from eastern Iraq totally entered Iran, and another dust mass formed in northwestern Iraq and eastern Syria. Also, the dust mass was shown in the southwest of Iran, which cannot be seen clearly due to the cloudiness in this area. At 12:00 UTC, a large part of southwestern and western Iran, the western and central hillsides of Alborz mountain range and the southern shores of the Caspian sea were affected by the dust. In addition, at this time, dust can be seen in areas of northern Iraq and central Iran. At 15:00 UTC, dust entered Turkmenistan from the Caspian Sea and was observed in the central regions of Iran. At 18:00 UTC, the dust mass in northern Iraq reached the border of Iran, and dust can be seen in almost all areas of Iran that are not covered by clouds.

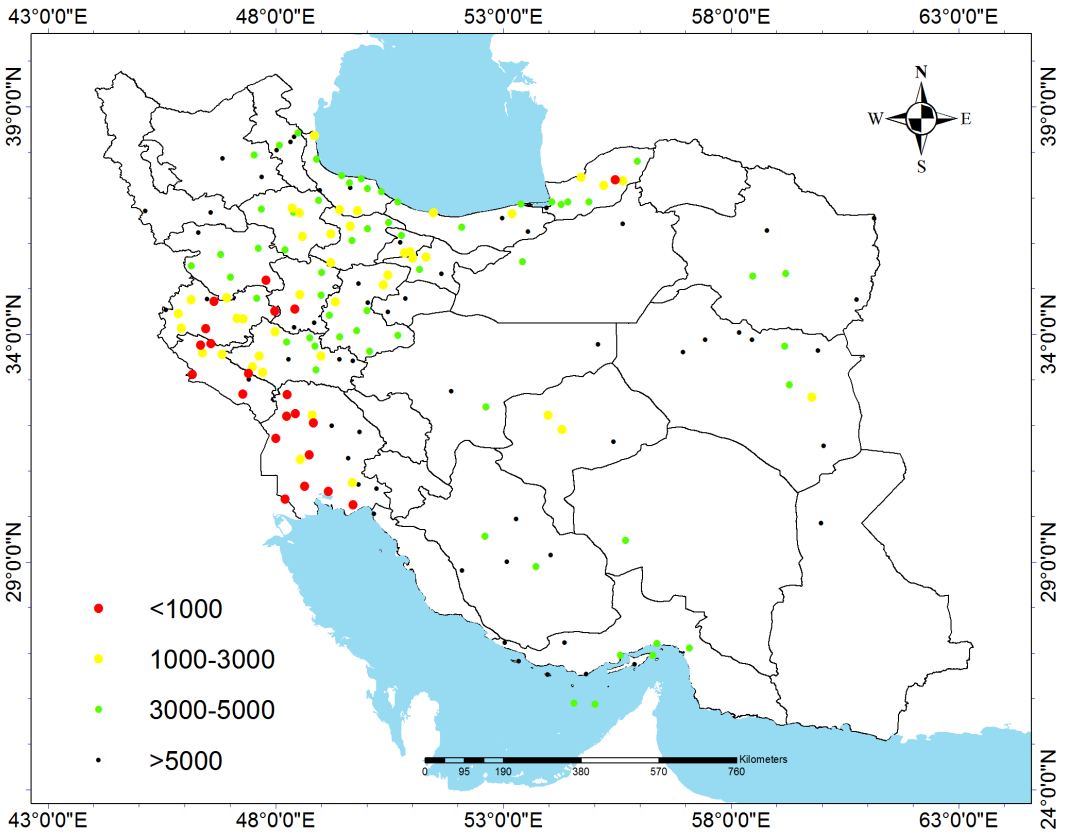

Fig. 3. Horizontal visibility of Iran synoptic stations with the dust phenomenon at 12 UTC on March 4, 2022

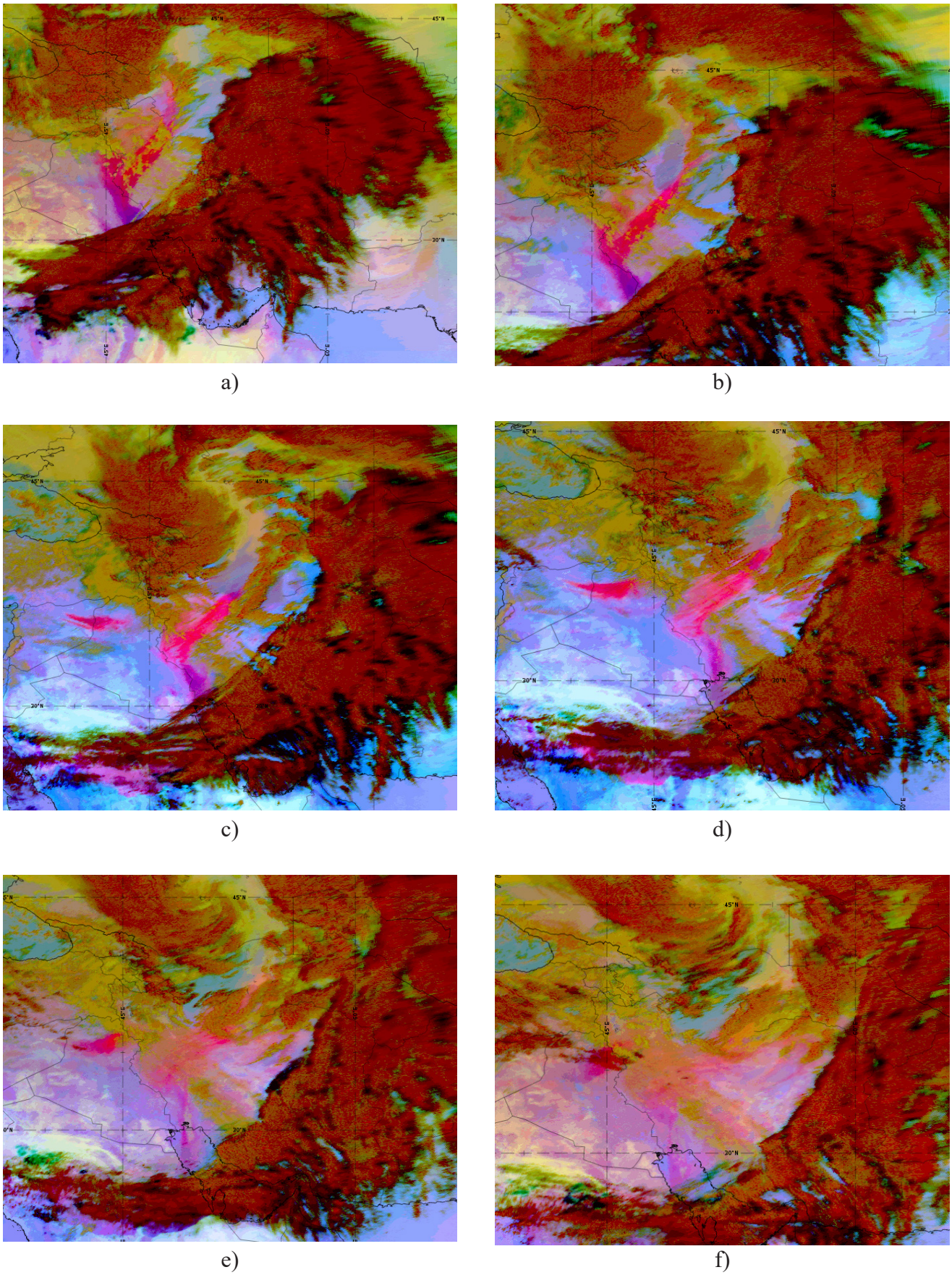

Fig. 4. Dust RGB image of MSG satellite on March 4, 2022 at a) 03, b) 06, c) 09, d) 12, h) 15 and f) 18 UTC

Fig. 5a shows the mean AOD on March from 2003 to 2022 and topographic contours. The highest average values of AOD are observed in the southeast of Iraq, the eastern half of Saudi Arabia and a large part of the Persian Gulf and its northern coasts that is in in agreement with the results of many previous studies. In a study the mean AOD values over the Middle east from 2002 until 2018 were analyzed and the results showed that High AOD values were seen in east Syria, vast parts of Iraq and Saudi Arabia, and over coastal areas of western Iran [40]. Also, in the average pattern, it can be seen that the Zagros heights in the western Iran have acted as a barrier against the penetration of dust particles into the central regions of the country. In a study to investigate the effect of the Zagros mountain range on dust, three numerical experiments were conducted using the WRF-Chem model [29]. One experiment in natural state, one in the state where the topography height is reduced to 1000 m and the other with complete removal of topography. In the third case, the dust concentration behind the Zagros mountain range decreased and the dust particles were transported to the central regions of Iran. Anyway, the AOD values decrease significantly after the height of about 1200 m (green meter).

The highest anomaly values of AOD on March 3 and 4, 2022 compared to the long-term average are observed in eastern Iraq, western and northwestern Iran, and a large part of the Caspian sea (Fig. 5b). It shows that in this case study, dust source located in the east of Iraq and the border region of Iran has been more active. It should be noted that the intense transport of dust particles from this region and reaching the Caspian Sea is not a common phenomenon.

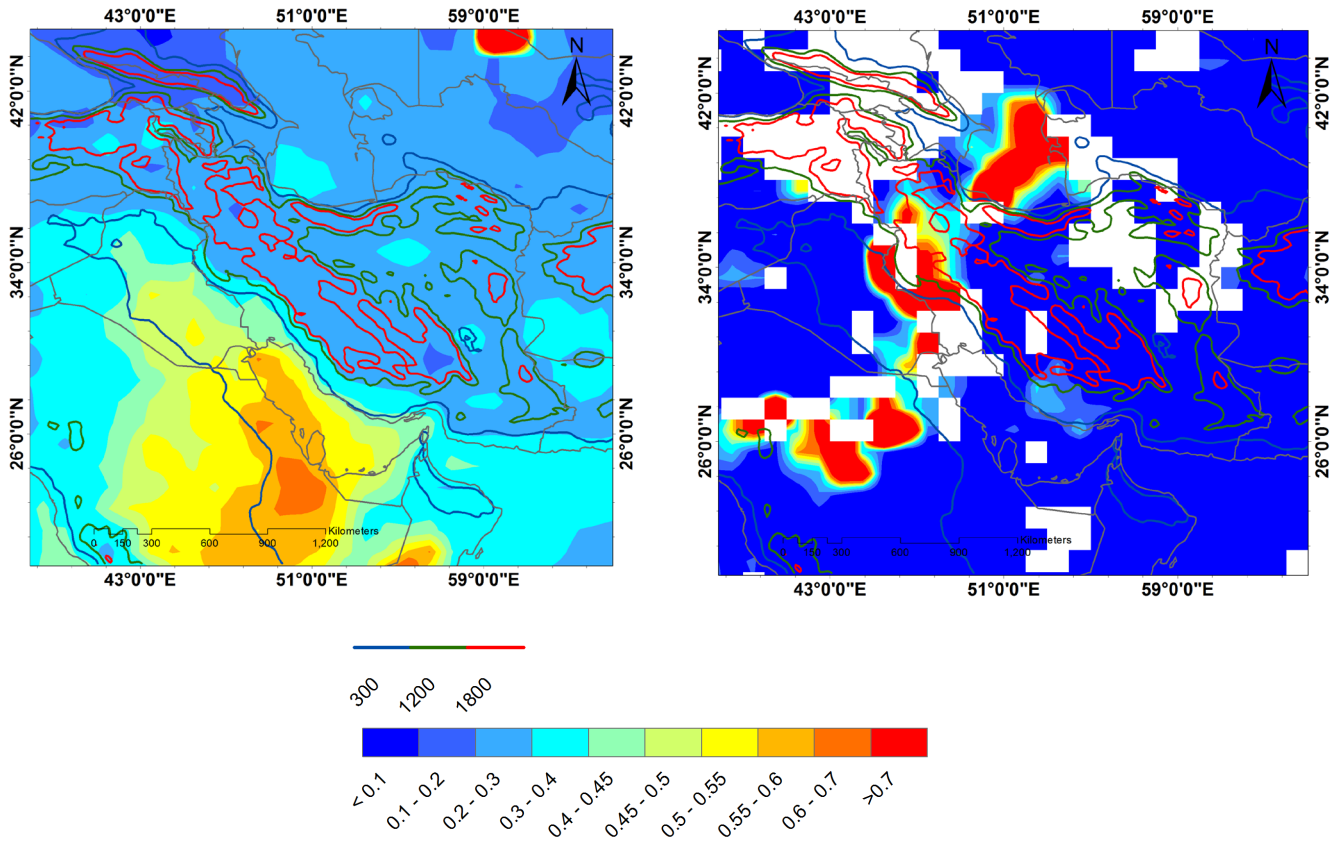

Fig. 5. a) The average optical thickness of aerosols on March 2003-2022 with topographic contours b) AOD anomaly on March 3 and 4, 2022 compared to the 20-year average (2003-2022)

Dust source area

According to the satellite images (Fig. 4) the dust moved from the source located in the east of Iraq, near the border of Iran, towards the Caspian Sea in this case study. In order to investigate from the climatic point of view of this dust phenomenon and the effective factors of its formation in the area (marked by the red square in Fig. 1), the monthly average of AOD and EVI index and also cumulative monthly precipitation on March from 2003 to 2022 is displayed in Fig. 6a. The highest AOD values were on March 2009 and 2018. On March 2022, AOD values were also significant. The lowest amount of precipitation was on March 2008 and 2018, in which year the AOD was also high. The lowest amount of vegetation (EVI index) is observed On March 2008, which also had the lowest amount of precipitation. The maximum values of vegetation was in 2019, where the highest amount of precipitation occurred. The correlation coefficient between AOD and EVI index is -0.43, and between AOD and precipitation is -0.36, which shows that the amount of AOD has increased with the decrease in precipitation or vegetation. The correlation coefficient between EVI index and rainfall is estimated as 0.66 and it shows that vegetation has also increased in rainy years. This is one of the characteristics of arid and semi-arid regions. The aerial image of the region in 2019 with maximum precipitation and vegetation and 2008 with minimum of these two quantities are shown in Figs. 6b and c. The comparison of these two images clearly shows the difference in the vegetation and surface waters of the region in these two years.

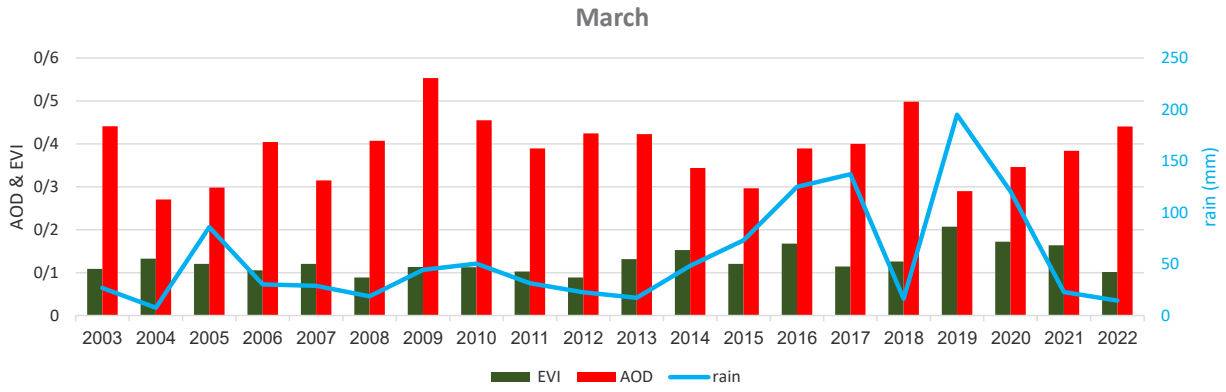

a)

b)

c)

Fig. 6. a) Monthly average of AOD, EVI index and monthly cumulative precipitation on March, 2003-2022; aerial image of the region in b) 2019 and c) 2008

The path of dust transfer

The True Color image of MODIS/Aqua on March 4, 2022 is shown in Fig. 7. As seen in the Dust RGB images, dust particles were transported in a path from the west of Iran and on the border of Iran and Iraq to the Caspian sea. The vertical profile of the height above the mean sea level in the dust transfer path (red line in Fig. 7) shows that in general, a large part of the path was located in mountainous areas, and even some areas were over 2250 m high, and there were valleys along the way with lower altitude. At the beginning of the mentioned line, at a distance of about 100 km from the starting point, there is a significant height increase. After rising from the surface, the dust particles ascended to a high altitude in the atmosphere and continued on their way by passing through the Zagros mountains. In Fig. 7b and c) the beginning and end part of the path can be seen in three dimensions. At the end of the path, the valley that is located around the city of Manjil and causes the channelization of air flow and strong local winds in this area is marked with a yellow arrow in the vertical profile (Fig. 7a). Manjil is one of the best locations in the world for installing wind turbine [41].

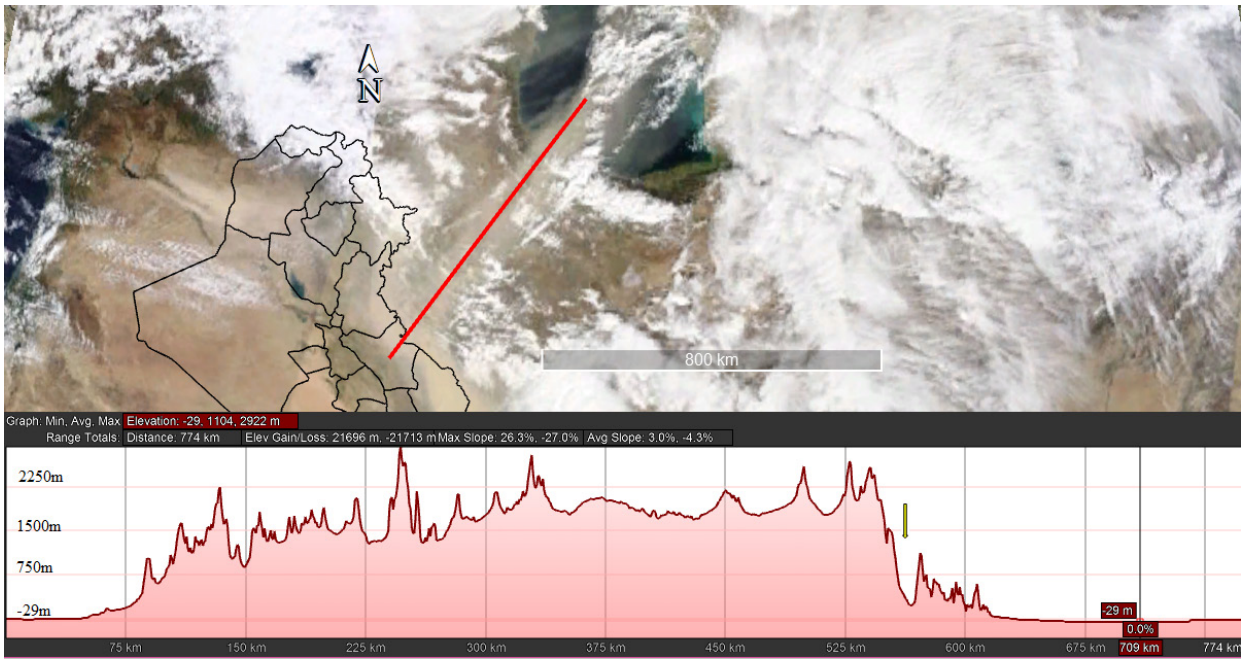

a)

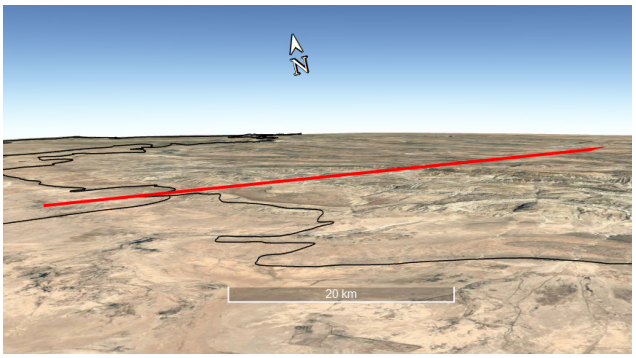

b)

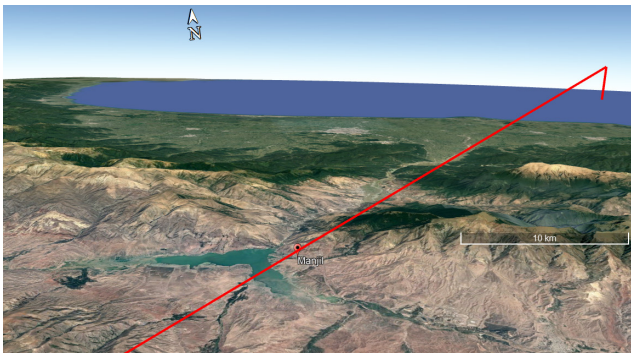

c)

Fig. 7. a) True color image of Aqua satellite's MADIS sensor on March 4, 2022. The red line shows the path of the vertical profile; and the three-dimensional image of b) the beginning, c) the end of the path

Synoptic analysis

Fig. 8 shows the Mean SLP and wind vector at hPa850 on March 3 and 4, 2022. At 12 UTC March 3, a low-pressure system was located over Iraq, continued towards northern Saudi-Arabia. Another low pressure was located in the east of Turkey, which was connected to the previous system. The other low pressure can be seen east of Black sea continued over Russia and reached the northwest of Iran and the west of the Caspian sea. Also, a high-pressure system spread over Africa to Northern Red sea and Jordan. The western parts of Turkey was also affected by high-pressure. The direction of the winds at this time was westerly over Iraq and south-westerly over Saudi Arabia (Fig. 8a). At 00 UTC on March 4th, with the strengthening and eastward motion of the high-pressure system, the low-pressure weakened over Iraq and was located in a small part of the southeast of Iraq, the west of the Persian Gulf, and the northeast of Saudi-Arabia. There was a significant increase in pressure over Turkey, especially in the western parts, and the low-pressure system in this region was greatly weakened. The low pressure over Russia strengthened, and surrounded a large part of northern Iran and joined the low pressure in the central areas of Iran. The direction of the winds was westerly in the north of Iraq and north-westerly in the south of country. In the north of Saudi Arabia, the direction of the winds was northwesterly and in the south it was south-westerly. (Fig. 8b). The change of wind direction in the west and north-west of Iran as well as south-east of Iraq and north-east of Saudi-Arabia indicates the existence of atmospheric fronts over these areas. In a study, 6 cases of frontal dust were investigated and simulated, and in all of them, a sudden change in the wind direction at the front location was observed [42].

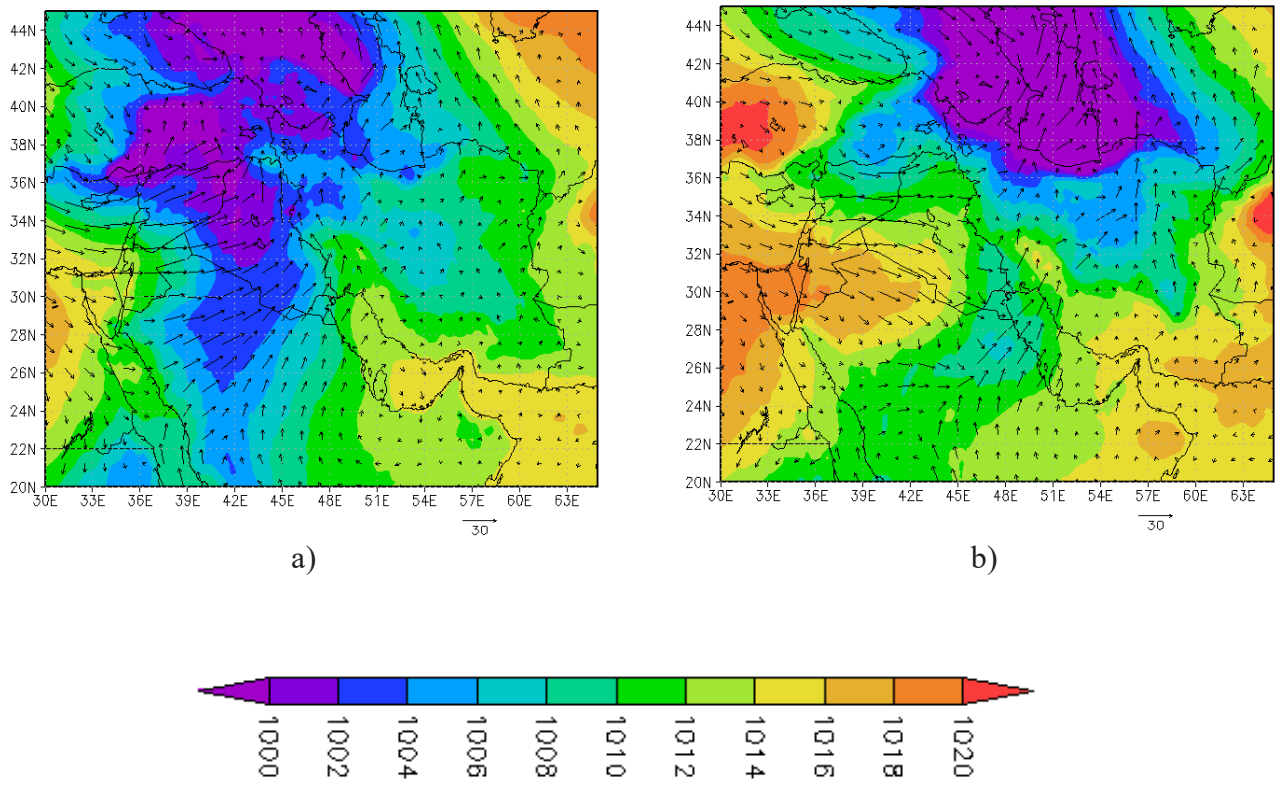

Fig. 8. Mean SLP (hPa) (Shaded) and wind vector at 850 hPa at a) 12 UTC on March 3th and b) 00 UTC on March 4th, 2022

In order to determine the position of atmospheric fronts, GPH and temperature at 850 hPa level are shown in Fig. 9. At 12 UTC on March 3, a low geopotential height system was located over Turkey and its trough reached southern Iraq and northern Saudi-Arabia. The trough of southeast Europe low geopotential height penetrated to northwest Iran. Over the border of Iran and Iraq, as well as in the west of Iran, miner trough can be seen, which indicate the northern currents and also significant upward motions in these areas. In the west of Turkey and north-east Africa, the ridge of GPH can be seen, which was associated with the high pressure system on the surface. As the trough moved eastward at 00 UTC on March 4, the northern half of Iran was affected. On this time, with the penetration of the cold air mass towards the east, the temperature gradient was significant in the east of Iraq and the west and north-west of Iran. The intense temperature gradient and advection of cold air confirm the existence of a cold front in these areas.

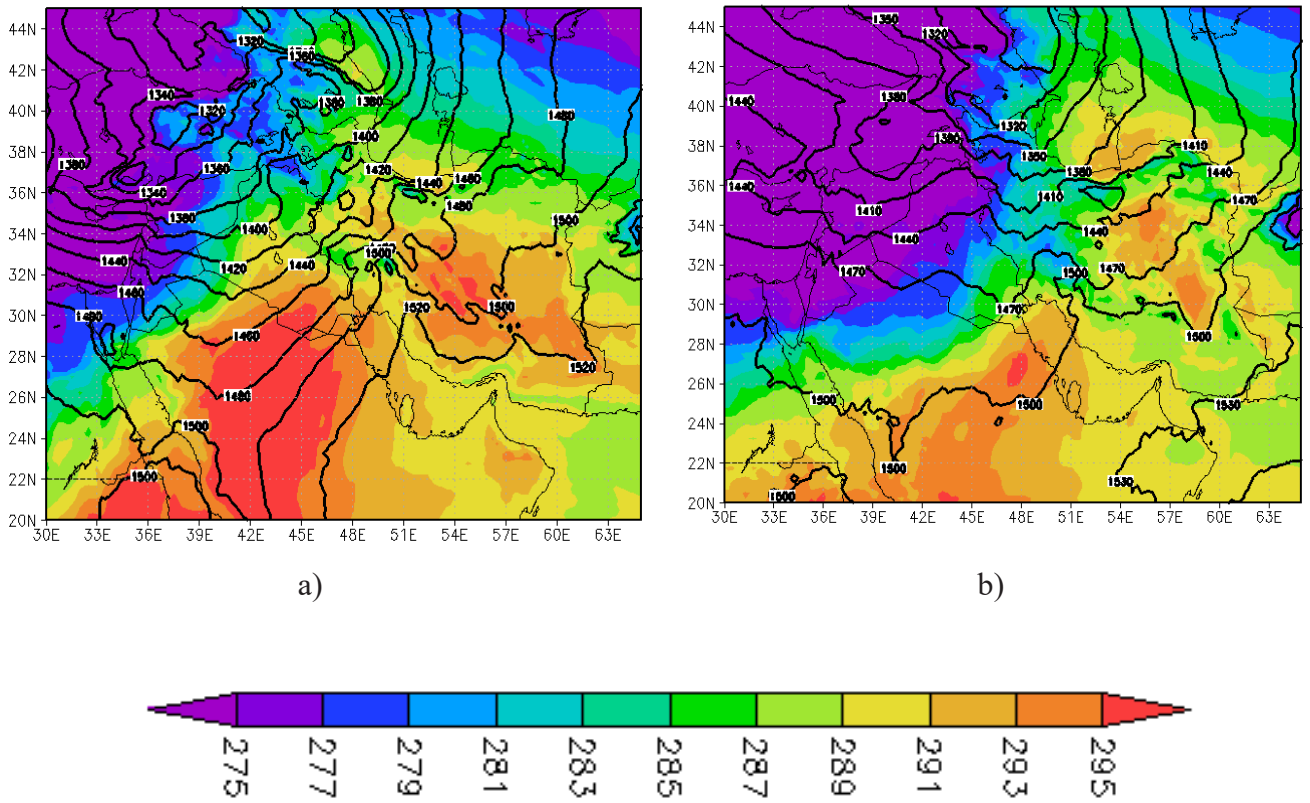

Fig. 9. GPH (meters) (bars) and temperature (K) (Shaded) at the 850 hPa level at a) 12 UTC on March 3th and b) 00 UTC on March 4th, 2022

Fig. 10 shows the True color image of the MODIS/Terra, the Isobars, winds at 850 hPa and the position of the atmospheric fronts on March 4, 2020. On this day, severe dust masses are observed behind the cold fronts on the southern shores of the Persian Gulf, southwestern Iran and southeastern Iraq. Also, another mass of dust stretched from eastern Iraq to the Caspian sea. Cloudiness associated with the cold front is observed in front of this dust mass. The presence of instability and strong upward motions in the location of the cold front in the absence of sufficient humidity caused the dust to be transported from the surface to the middle levels of the atmosphere. Therefore, the transfer of dust particles from the east of Iraq to the Caspian sea and from the top of the high mountains was due to the presence of a cold front in the region. Of course, as discussed before, topographical effects also played an important role in determining the path of particle transport, especially when particles passed through the Alborz mountain range and entered the Caspian sea.

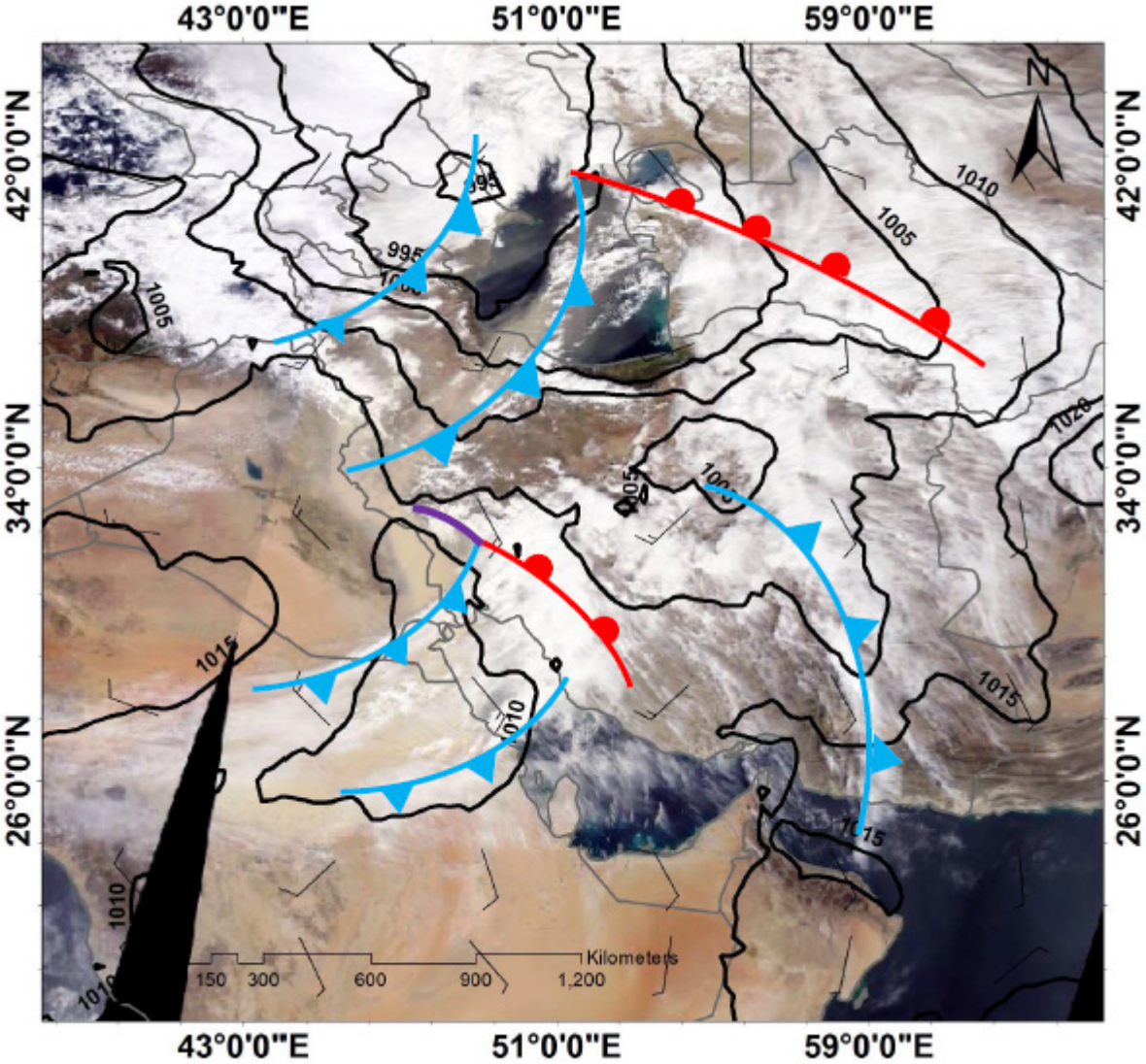

Fig. 10. True color image of Terra satellite's MADIS sensor, Isobars (contours), wind at 850 hPa and the position of atmospheric fronts on March 4, 2020

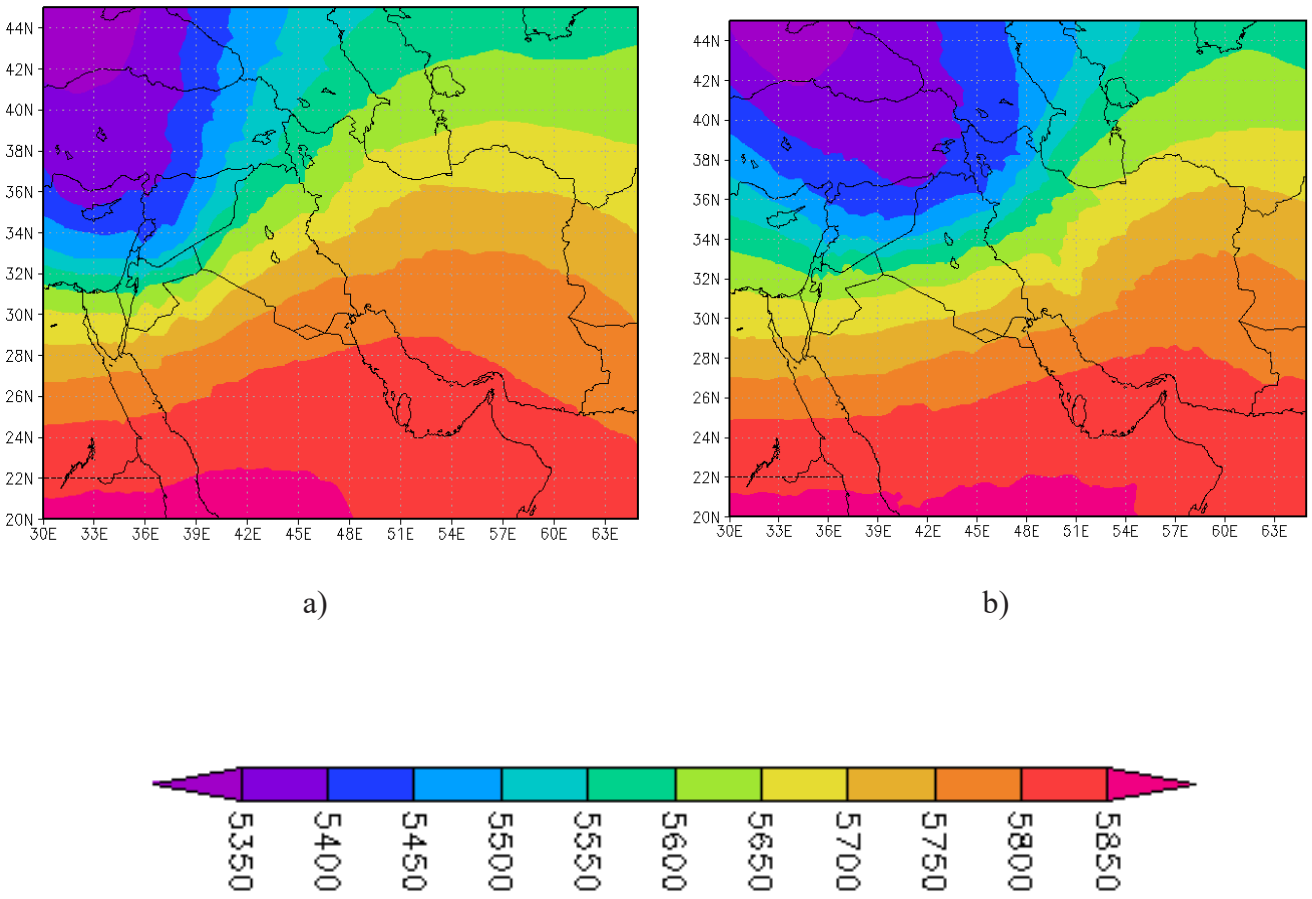

Fig. 11. GPH of 500 hPa (m) at a) 12 UTC on March 3, b) at 00 UTC on March 4, 2022

The GPH of 500 hPa in Figure 11 shows that at 12 UTC on March 3, the trough extended over the southeast of Europe to the north of Saudi-Arabia in such a way that the east of Iraq and the northwest of Iran were in the east of trough and were affected by the northern currents and upward motions. On the other hand, the ridge penetrated from low latitudes to the country of Turkmenistan. At 00 UTC on March 4, the trough moved to the east, and its axis was slightly tilted and was located in the northwest-southeast direction. Significant height gradient can be observed in the western and northwestern regions of Iran.

Fig. 12 shows vertical velocity in pressure coordinates (Omega) and LI at 850 hPa, Absolute vorticity at hPa700 level and wind speed at 300 hPa at 12 UTC on March 3th. Omega values were negative in a large part of the eastern half of Iraq, especially in the northeast of country and near the Iranian border, which indicates the presence of upward movements in this region. The negative values of Omega on the Zagros mountain range also indicate the upward movements that caused the dust to be transported to the upper altitudes of the atmosphere. On the southern shores of the Caspian sea, Omega was positive, which indicates the downward movement and subsidence of dust in these areas (Fig. 12a). The surface LI index (best 4 layers) shows the lowest values (less than -6) over the Red sea, which indicates very unstable conditions and

the possibility of forming a severe storm in this area. In northern Saudi-Arabia, south-eastern Iraq and western Iran, LI values were between -2 and -4, which indicates unstable conditions and the possibility of storm formation in these areas. The presence of instability in these areas strengthened the upward movement and vertical transfer of dust particles (Fig. 12c). Absolute vorticity amounts at 700 hPa were positive in a large part of the northern half of Iraq and western Iran, which indicates upward movements on these areas and at this atmospheric level as well. On the south of the Caspian sea, the negative values of vorticity indicate the descent of air in these areas. The wind field at 300 hPa shows the core of the polar jet over North-East Africa, areas of the Mediterranean, Jordan and North-West Saudi-Arabia. In the west of Iraq to the north-west of Iran, the component of the meridional wind speed was significant, and in these areas, the jet stream was in the southwest-northeast direction.

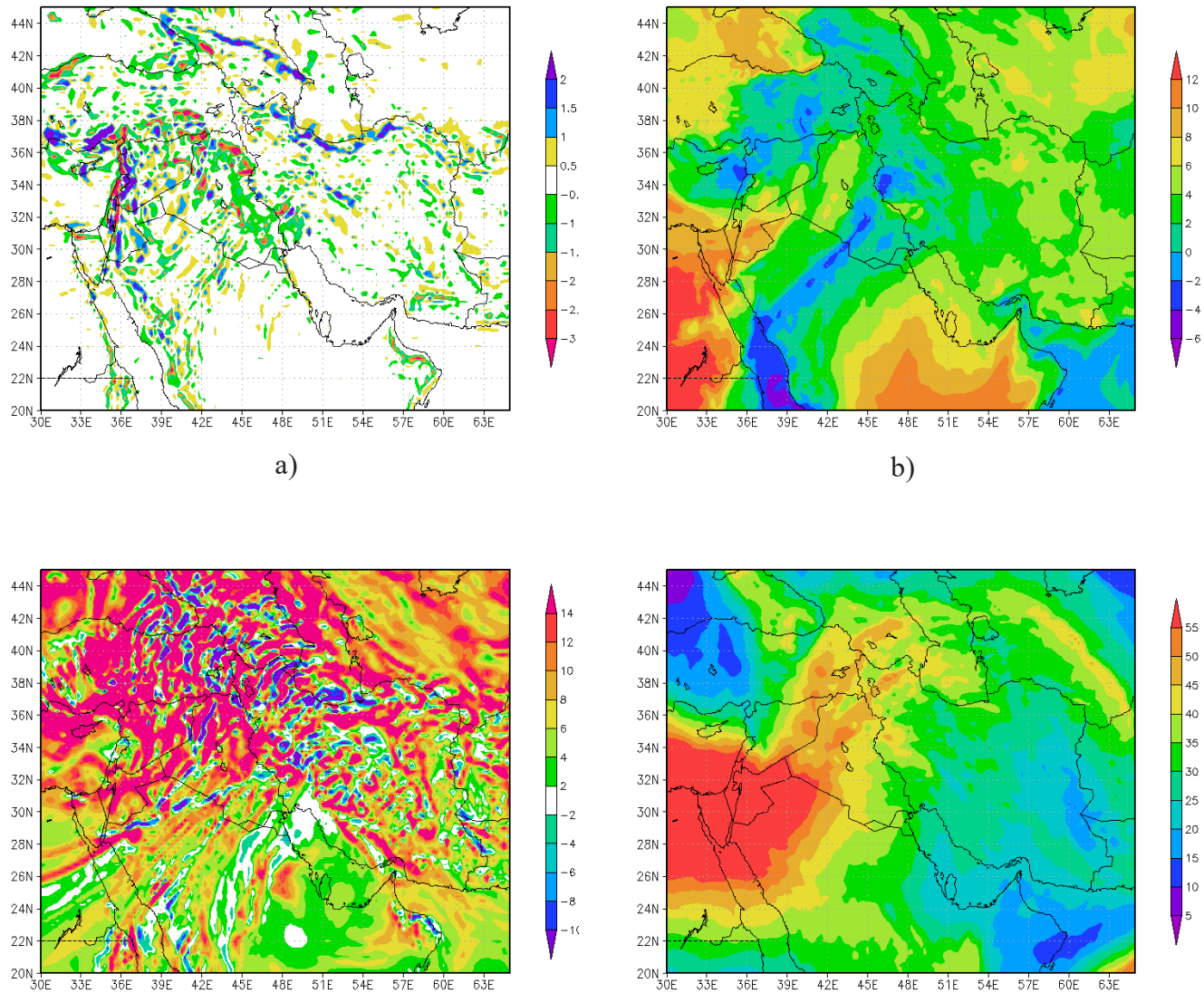

Fig. 12. a) Vertical velocity in pressure coordinates, b) LI at 850 hPa, c) Absolute vorticity (10e5) at 700 hPa and d) Wind speed at 300 hPa at 12 UTC on March 3, 2022

The anomaly of Mean SLP, GPH, Omega and wind speed at 850 hPa and GPH at 500 hPa on March 3, 2020 compared to long-term 1981-2010 can be seen in Fig. 13. Mean SLP anomaly was negative in a large part of the region, so that its value was less than -16 hPa in eastern Turkey, the Black sea and some parts of south-east Russia. In addition, the anomaly of Mean SLP over the countries of Iraq and Syria, northern Saudi-Arabia, the Caspian sea and the northern half of Iran was lower than the climatic average on this day (Fig. 13a). The GPH anomaly at 850 hPa was negative over Turkey, Iraq, Syria, North-West and west of Iran and north of Saudi Arabia, which indicates a sharp decrease in GPH in these areas compared to the long-term average. On the other hand, positive values of geopotential height anomaly are observed in the eastern and southern half of Iran (Fig. 13b). The negative anomaly of Omega from the east of Syria to the west and south-west of Iran indicates the strengthening of upward movements in the mentioned areas at this day compared to the long-term average. The positive anomaly of Omega over the Caspian sea indicates more severe downward movements compared to the climatic average (Fig. 13b). The anomaly of the wind speed at 850 hPa (shaded) was positive over Syria, Iraq, Jordan, northern Saudi-Arabia and western Iran, which shows that the wind speed in these areas was higher than the 30-year average. On the other hand, the positive anomaly of the meridional wind component (black lines) in these areas indicates strong southerly currents on this day (Fig. 13c). The negative anomaly of the GPH of 500 hPa is evident over the Black sea, the eastern Mediterranean sea, Turkey, Syria and western Iraq and the significant positive anomaly over Iran and south-eastern Iraq (Fig. 13d).

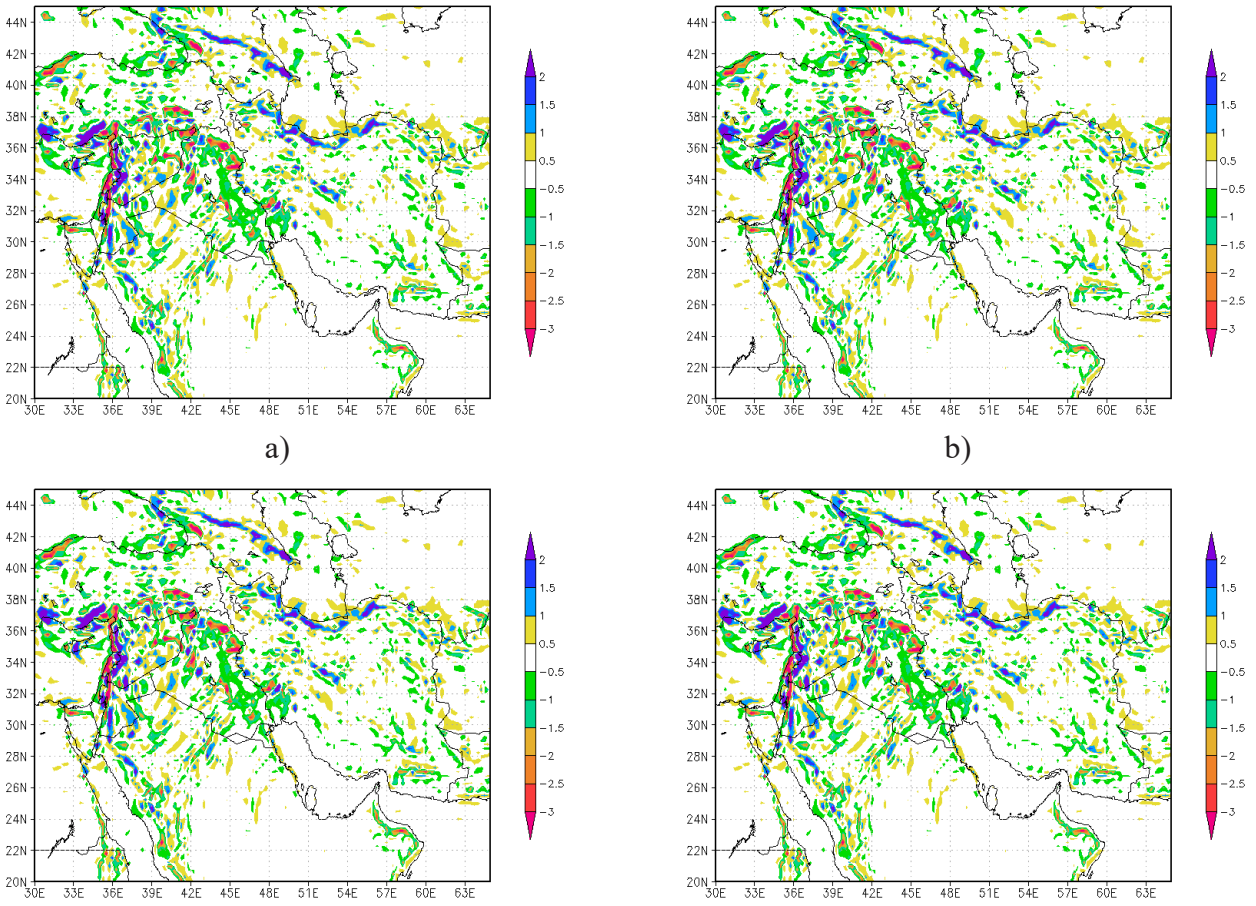

Fig. 13. Anomaly of the a) Mean SLP b) GPH (shaded) and omega (black lines) at 850 hPa, c) wind speed (shaded) and its meridional component (black lines) at 850 hPa and d) GPH of 500 hPa on March 3, 2020 compared to the 30-year average (1981-2010)

Trajectory and dispersion of dust particles

The HYSPLIT model was used to investigate the trajectory and dispersion of dust particles. The output of the HYSPLIT trajectory model at 03 UTC on March 4, 2022, is shown in Fig. 14. The model was implemented in a matrix from an area located in the east of Iraq and near the border of Iran, in a forward manner for 24 h at an altitude of 500 m. As it is clear from the figure, southwesterly currents prevail in the northern part of the area and the dust particles of this area were transported towards the Caspian sea. Northwesterly currents from the southern part transferred the dust particles towards the southwest Iran and the Persian Gulf.

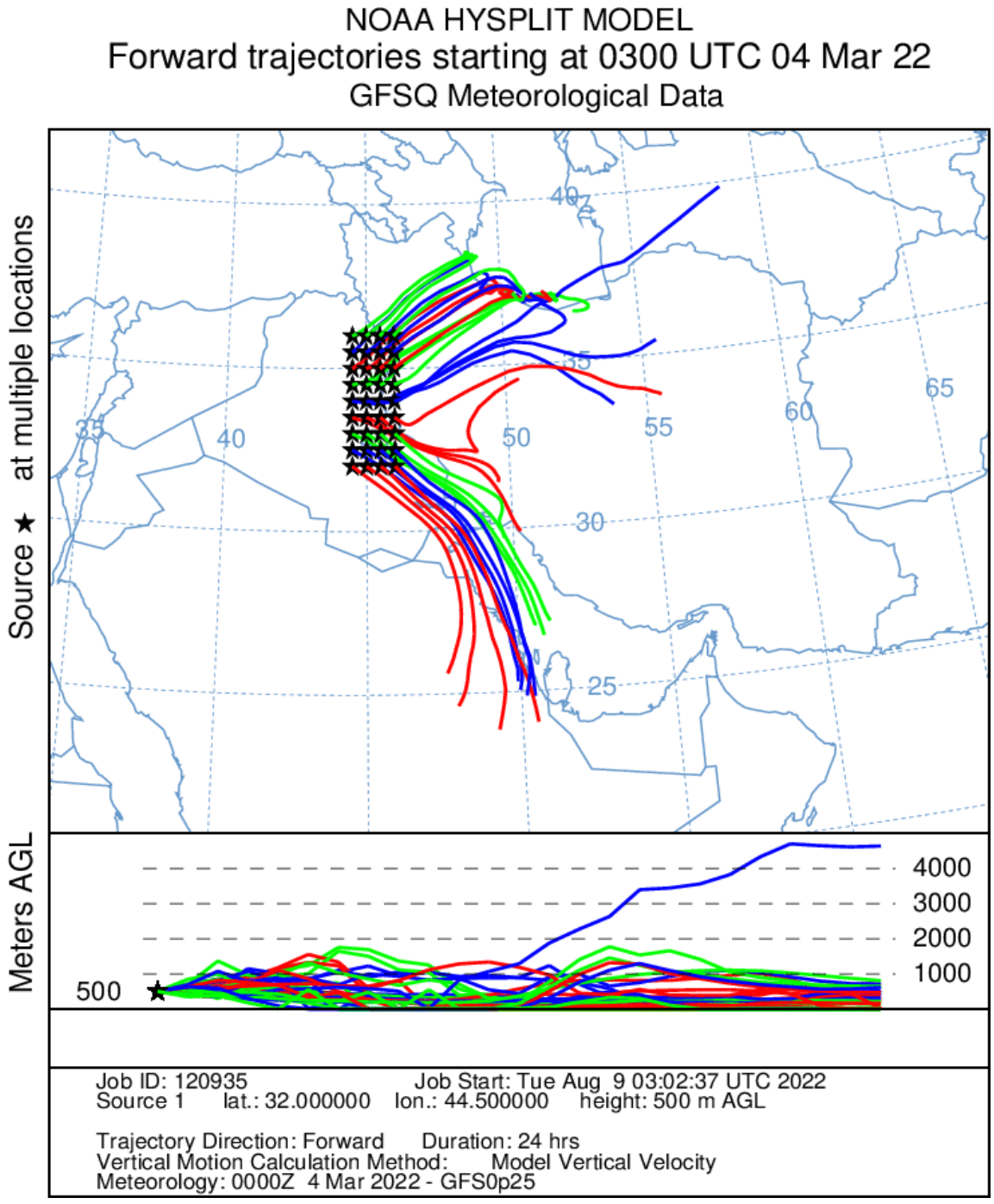

Fig. 14. HYSPLIT trajectory model output at 03 UTC on March 4, 2022

Also, the output of the HYSPLIT dispersion model, which was implemented from a point located in the east of Iraq, near the border of Iran (Fig. 15), shows that near the area of the dust source, the particles were located at a height of less than 3 km. At a short distance from the starting point on the Zagros mountain range, the penetration height of particles reached 6 km. Near the Alborz mountain range and in the north-eastern regions of Iran and Turkmenistan, the height of the particles reached 9 km. The time analysis shows that after about 4 h from the start of the performance, the dust particles passed through the Zagros mountains and moved towards the Caspian sea. About 8 h after the start of the implementation, the particles reached the southern shores of the Caspian sea, and after that, the transfer of particles continued towards the north-east of Iran and Turkmenistan.

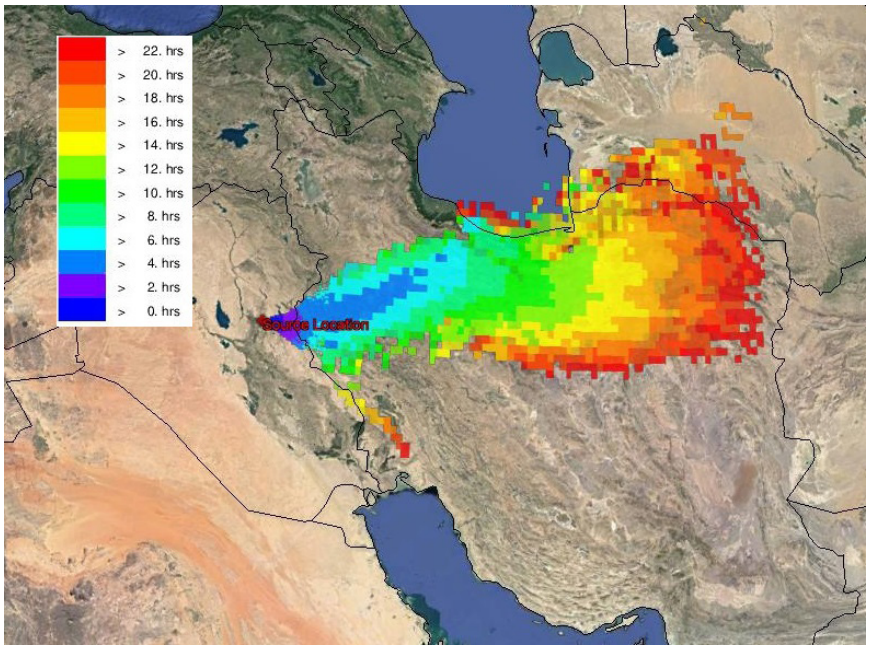

a)

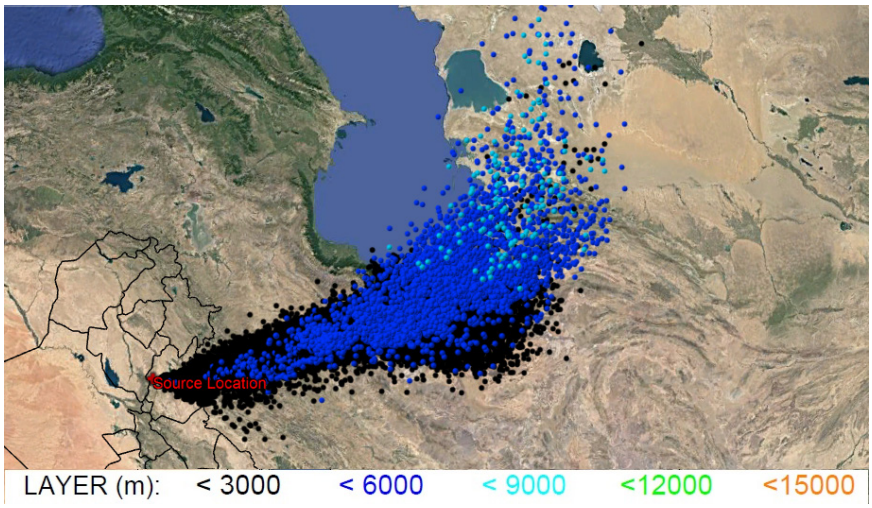

b)

Fig. 15. HYSPLIT Dispersion model output at 03 UTC on March 4, 2022

Simulation by the WRF-Chem model

Fig. 16 shows the output of surface dust concentration and wind at 850 hPa of the WRF-Chem model and along with topographic contours. At 1500 UTC on March 3, three strong dust masses are observed in Iraq. The first dust mass was located on the border of Iraq and Syria, the second was in the west of Iraq and the third was in the east of Iraq and near the border of this country with Iran. At this time, westerly winds were blowing in the western half of Iraq, which caused dust to be transferred to the central regions of this country. The blowing of southern winds in the eastern half of Iraq moved the dust present in this region to higher latitudes (Fig. 16 a). At 0000 UTC on March 4, the dust in the western regions of Iraq was transferred to the central and southern areas of this country and due to the northerly winds, they entered the border regions of Saudi Arabia in the north of this country. On the other hand, the dust in the east of Iraq entered the west of Iran due to the south-westerly winds and passing through the Zagros highlands, it was moving towards the west coast of the Caspian sea. In the northwest of Iran, the concentration of dust after the height of 1800 m (red lines) has shown a slight decrease, which can be caused by the effect of heights in preventing the passage of some dust particles (Fig.16b). At 0600 UTC on March 4, dust particles were transported to the Caspian sea. Dust entered the Caspian sea from an area that has a lower altitude than other areas (Manjil Valley) (Fig. 16c). At 1200 UTC on March 4, the concentration of dust in the region decreased, especially in the heights of Zagros, but dust is still visible on the eastern coast of the Caspian sea (Fig. 16d).

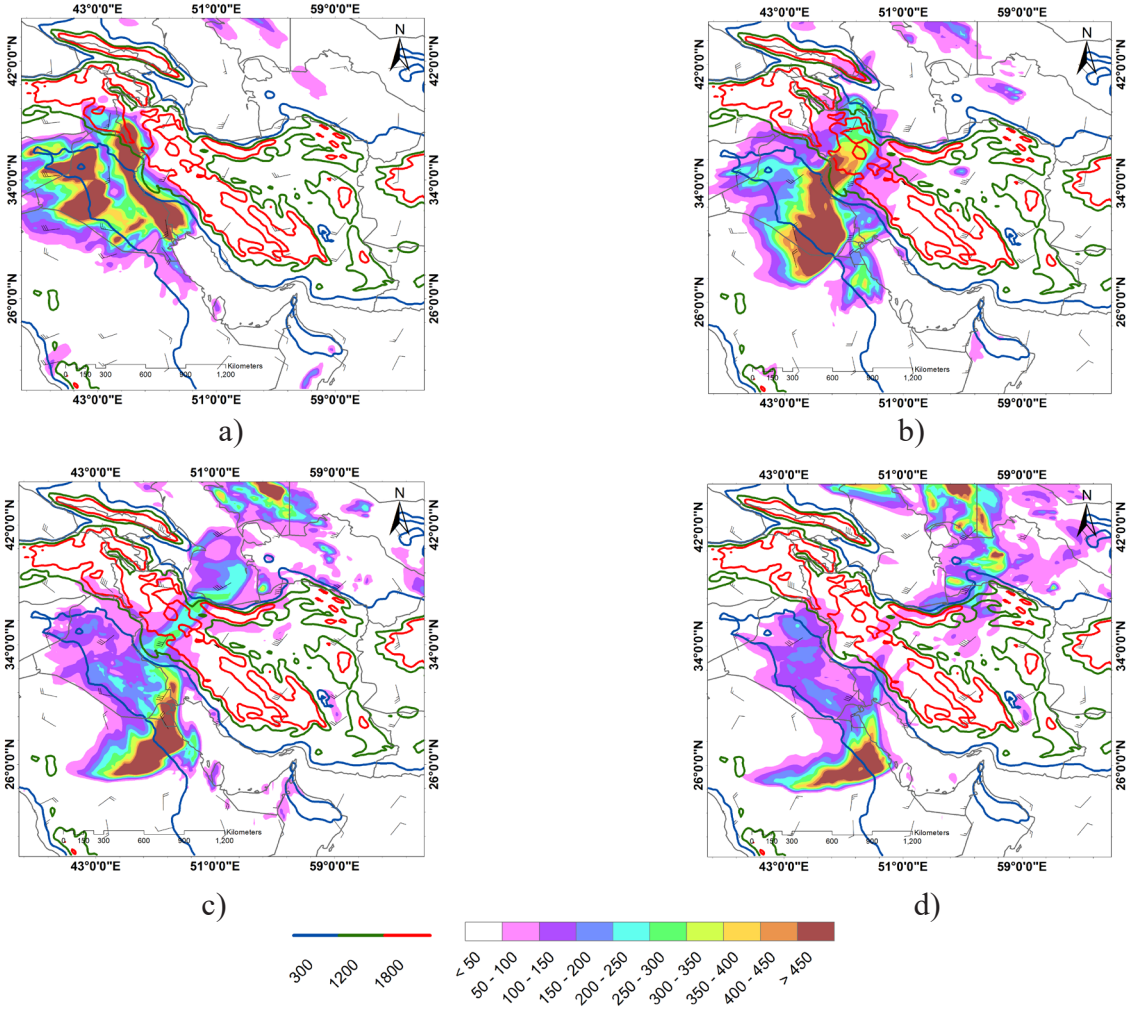

Fig. 16. The output of surface dust concentration and wind at 850 hPa of the WRF-Chem and height contours at a) 1500 UTC on March 3, b) 0000 UTC, c) 0600 UTC and d) 1200 UTC on March 4, 2022

The vertical cross-section of dust concentration, relative humidity percentage and wind speed of WRF-Chem model output on a line from the center of Iraq to the east of the Caspian Sea in Turkmenistan (yellow line) is shown in Fig. 17. At 1500 UTC on March 3, dust is observed around the starting point of the path located in Iraq. The concentration of dust behind the mountainous area was significant due to the proximity to the dust source located in eastern Iraq and the accumulation of dust. In this area, the particles raised up to the level of 600 hPa and could pass over the heights. The negative slope of wind speed contours (black lines) indicates an increase in wind speed in this area compared to nearby areas. High amounts of relative humidity (blue lines) over the mountains (about 90%) indicate the presence of clouds in this region. At 2100 UTC on March 3, the concentration of dust behind the topography and above the mountains greatly increased. An increase in relative humidity and a significant wind speed gradient right in front of the dust mass are signs of the front. At 0300 UTC on March 4, dust spread in a large part of the region and on the heights, but its concentration decreased. At 0900 UTC on March 4, the reduction of dust concentration in the whole region was significant. Therefore, the legend of concentration values was changed in such a way that the distribution of particles can be seen. At this time, dust can be seen on the entire path, but in its final part on the Caspian sea and western Turkmenistan, the highest concentration is observed and the dust particles raised to higher altitudes. The surface wind speed in this area reached about 60 knots. At 1200 UTC on the same day, the dust concentration decreased over the highlands and the Caspian sea, but dust with a high concentration is still observed over Turkmenistan in the middle levels (between the levels of 750 and 500 hPa).

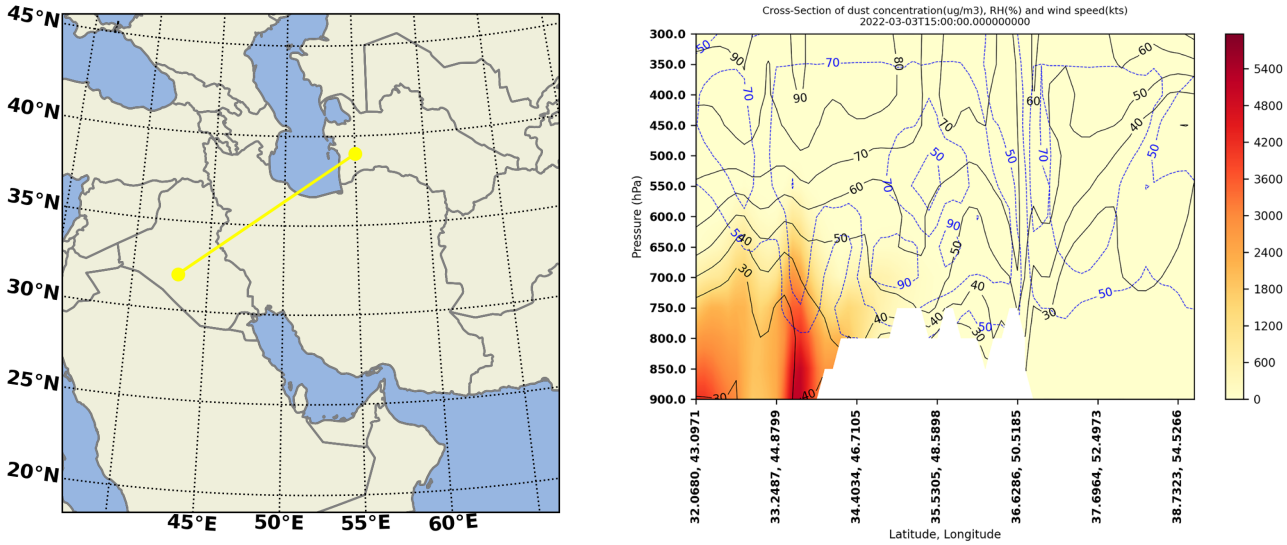

a) b)

Fig. 17. a) The path of the vertical profile and the vertical cross-section of the dust concentration output (colored sections), relative humidity percentage (blue lines) and wind speed (black lines) of the WRF-Chem model at b) 15 UTC, c) 21 UTC on March 3 and d) 03 UTC, e) 09 UTC and f) 12 UTC on March 4, 2022

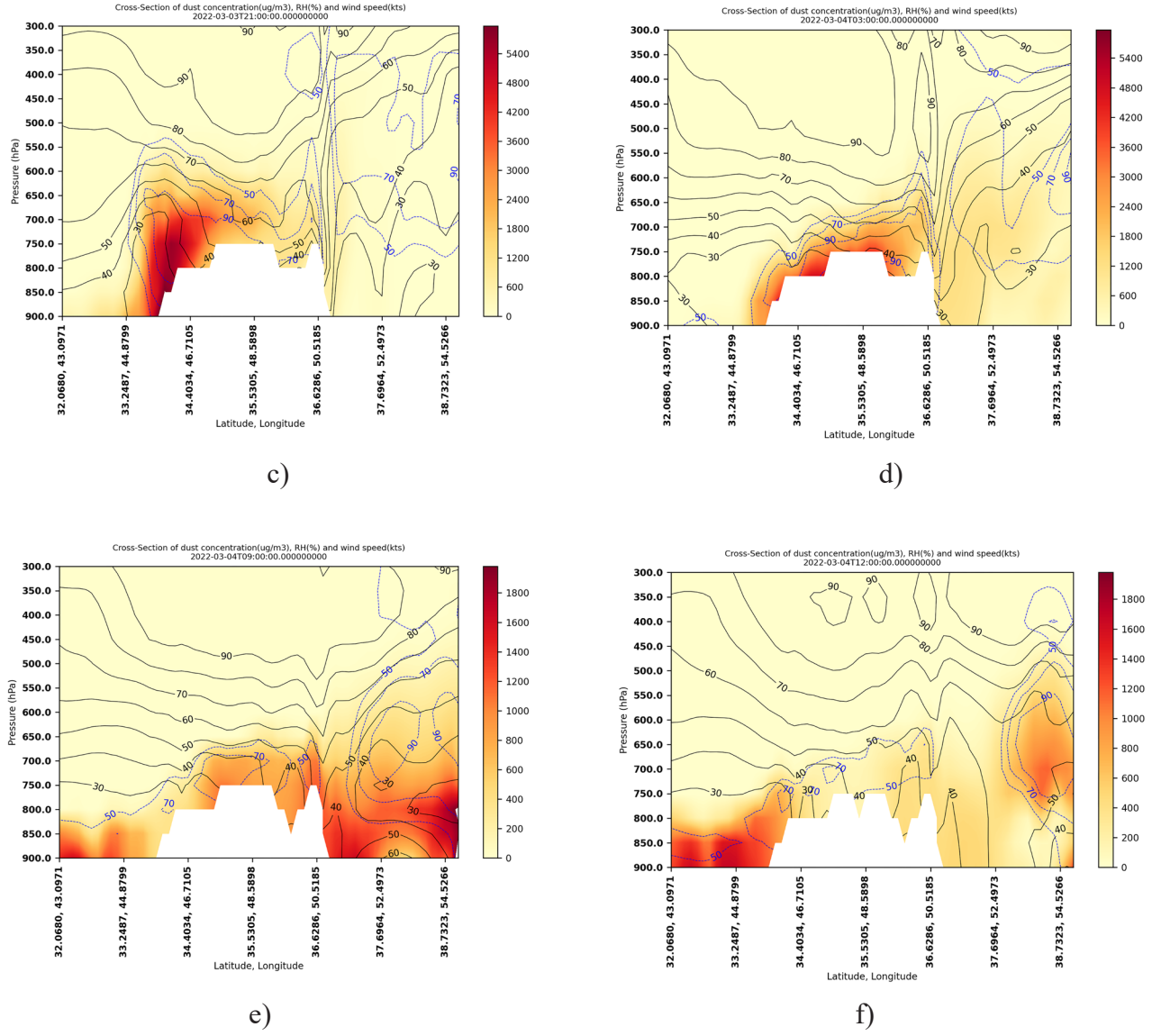

Fig. 17. a) The path of the vertical profile and the vertical cross-section of the dust concentration output (colored sections), relative humidity percentage (blue lines) and wind speed (black lines) of the WRF-Chem model at b) 15 UTC, c) 21 UTC on March 3 and d) 03 UTC, e) 09 UTC and f) 12 UTC on March 4, 2022

Conclusion

In this study, a severe dust storm on March 3 and 4, 2022, in which several dust masses from dust centers in the countries of Syria, Iraq, Kuwait, southwest Iran and even the plains in the south of central Alborz (due to two-year drought) were active according to satellite images, was investigated and simulated. Of course, the focus of this study is on the dust mass that was emitted from the sources located in the east of Iraq, near the border of Iran and entered the west and north-west regions of Iran and the Caspian sea by passing through the Zagros and Alborz mountains due to the southerly and south-westerly winds.

The anomaly of AOD on March 3 and 4, 2022, was more than the long-term average. The main factors of the formation of this Unconventional dust, in which the particles have been transferred to the Caspian sea contains: severe two-year drought in the Middle East, reduction of vegetation and cold front related to the dynamic

low-pressure system located in the east of the Black sea, east of Turkey, Syria and parts of northern Iraq then, which in the following hours have moved eastward to the Caspian sea. Examining the anomaly values of some meteorological quantities indicate a decrease in the Mean SLP and the severity of the pressure gradient in a large part of the studied area compared to the long-term, an increase in the horizontal and vertical wind speed, as well as a positive and severe anomaly of the Meridional component of wind at 850 hPa. The intensity of the instability and upward movement was such that the dust particles in the source area raised to the middle levels of the atmosphere and in a short distance, a large part of the particles passed through the Zagros mountains.

There is a valley in the western part of the Alborz mountain range (Qazvin Rasht road) where the city of Manjil is located. The existence of this valley in the middle of the heights causes the air flow to be channeled and very strong winds to blow in this area. Examining the path of dust particle transmission in this study case show that a large part of dust particles passed through this valley and penetrated to the Caspian sea.

According to the output of the HYSPLIT model, dust particles were transported from eastern Iraq to the Caspian sea in less than 12 h, which was the result of strong winds in the region. The simulation of this dust phenomenon with the WRF-Chem numerical model shows the dust was transported from the east of Iraq to the Caspian sea as well as the dust particles passed over the heights. Also, the vertical profile shows the ascent of dust particles up to the level of 600 hPa near the dust source and its passage over mountainous areas.

Financial supports

This study does not have any financial support.

Competing interests

The authors declare that there are not any actual or potential competing interests.

Acknowledgements

The GDAS/FNL reanalysis teams are gratefully acknowledged for providing the meteorological maps and running WRF-Chem model. The authors also thankful for AOD, EVI and the cumulative precipitation data retrieved via Giovanni (https://giovanni.sci.gsfc.nasa.gov/giovanni/). We thank EUMETSAT for Dust RGB images of MSG satellite.

Ethical considerations

Ethical issues (Including plagiarism, Informed Consent, misconduct, data fabrication and/or falsification, double publication and/or submission, redundancy, etc) have been completely considered by the authors.

References

1. Griffin DW, Kellogg CA. Dust storms and their impact on ocean and human health: dust in Earth's atmosphere. EcoHealth. 2004 Sep;1(3):284-95.

2. Derbyshire E. Natural minerogenic dust and human health. AMBIO: A Journal of the Human Environment. 2007 Feb;36(1):73-7.

3. Khaniabadi YO, Daryanoosh SM, Amrane A, Polosa R, Hopke PK, Goudarzi G, Mohammadi MJ, Sicard P, Armin H. Impact of Middle Eastern Dust storms on human health. Atmospheric pollution research. 2017 Jul 1;8(4):606-13.

4. Baddock MC, Strong CL, Murray PS, McTainsh GH. Aeolian dust as a transport hazard. Atmospheric environment. 2013 Jun 1;71:7-14.

5. Middleton NJ. Desert dust hazards: A global review. Aeolian research. 2017 Feb 1;24:53-63.

6. Kazem AA, Chaichan MT, Kazem HA. Dust effect on photovoltaic utilization in Iraq. Renewable and Sustainable energy reviews. 2014 Sep 1;37:734-49.

7. Sarver T, Al-Qaraghuli A, Kazmerski LL. A comprehensive review of the impact of dust on the use of solar energy: History, investigations, results, literature, and mitigation approaches.

Renewable and sustainable energy Reviews. 2013 Jun 1;22:698-733.

8. Al-Hemoud A, Al-Dousari A, Misak R, Al-Sudairawi M, Naseeb A, Al-Dashti H, Al-Dousari N. Economic impact and risk assessment of sand and dust storms (SDS) on the oil and gas industry in Kuwait. Sustainability. 2019 Jan 3;11(1):200.

9. Zhang XY, Gong SL, Zhao TL, Arimoto R, Wang YQ, Zhou ZJ. Sources of Asian dust and role of climate change versus desertification in Asian dust emission. Geophysical Research Letters. 2003 Dec;30(24).

10. Lababpour A. The response of dust emission sources to climate change: Current and future simulation for southwest of Iran. Science of The Total Environment. 2020 Apr 20;714:136821.

11. Karami S, Kaskaoutis DG, Kashani SS, Rahnama M, Rashki A. Evaluation of nine operational models in forecasting different types of synoptic dust events in the Middle East. Geosciences. 2021 Nov 7;11(11):458.

12. Middleton N, Kashani SS, Attarchi S, Rahnama M, Mosalman ST. Synoptic causes and socio-economic consequences of a severe dust storm in the Middle East. Atmosphere. 2021 Oct 30;12(11):1435.

13. Al-Jumaily KJ, Ibrahim MK. Analysis of synoptic situation for dust storms in Iraq. Int. J. Energ. Environ. 2013;4(5):851-8.

14. Wang W, Fang Z. Numerical simulation and synoptic analysis of dust emission and transport in East Asia. Global and planetary change. 2006 Jul 1;52(1-4):57-70.

15. Tan Z, Liu Y, Zhu Q, Shao T. Impact of massive topography on the dust cycle surrounding the Tibetan Plateau. Atmospheric Environment. 2021 Nov 1;264:118703.

16. Hoffmann C, Funk R, Wieland R, Li Y, Sommer M. Effects of grazing and topography on dust flux and deposition in the Xilingele grassland, Inner Mongolia. Journal of arid environments. 2008 May 1;72(5):792-807.

17. Heisel M, Chen B, Kok JF, Chamecki M. Gentle topography increases vertical transport of coarse dust by orders of magnitude. Journal of Geophysical Research: Atmospheres. 2021 Jul 27;126(14):e2021JD034564.

18. Moridnejad A, Karimi N, Ariya PA. Newly desertified regions in Iraq and its surrounding areas: Significant novel sources of global dust particles. Journal of Arid Environments. 2015 May 1;116:1-0.

19. Engelbrecht JP, Jayanty RK. Assessing sources of airborne mineral dust and other aerosols, in Iraq. Aeolian Research. 2013 Jun 1;9:153-60.

20. Abdi Vishkaee F, Flamant C, Cuesta J, Oolman L, Flamant P, Khalesifard HR. Dust transport over Iraq and northwest Iran associated with winter Shamal: A case study. Journal of Geophysical Research: Atmospheres. 2012 Feb 16;117(D3).

21. Yu Y, Notaro M, Kalashnikova OV, Garay MJ. Climatology of summer Shamal wind in the Middle East. Journal of Geophysical Research: Atmospheres. 2016 Jan 16;121(1):289-305.

22. Francis DB, Flamant C, Chaboureau JP, Banks J, Cuesta J, Brindley H, Oolman L. Dust emission and transport over Iraq associated with the summer Shamal winds. Aeolian Research. 2017 Feb 1;24:15-31.

23. Hamzeh NH, Karami S, Kaskaoutis DG, Tegen I, Moradi M, Opp C. Atmospheric dynamics and numerical simulations of six frontal dust storms in the Middle East region. Atmosphere. 2021 Jan 18;12(1):125.

24. Hamidi M. Atmospheric investigation of frontal dust storms in Southwest Asia. Asia-Pacific Journal of Atmospheric Sciences. 2019 May;55(2):177-93.

25. Giannakopoulou EM, Toumi R. The Persian Gulf summertime low-level jet over sloping terrain. Quarterly Journal of the Royal Meteorological Society. 2012 Jan;138(662):145-57.

26. Najafi MS, Sarraf BS, Zarrin A, Rasouli AA.

Climatology of atmospheric circulation patterns of Arabian dust in western Iran. Environmental monitoring and assessment. 2017 Sep;189(9):1-3.

27. Malakooti H, Babahoseini S. Formation and Evolution of a heavy dust storm over Middle East: A Numerical Case Study. Journal of Geography and environmental hazards. 2015 Jan 21;3(4):53-65.

28. Abdi Vishkaee F, Flamant C, Cuesta J, Flamant P, Khalesifard HR. Multiplatform observations of dust vertical distribution during transport over northwest Iran in the summertime. Journal of Geophysical Research: Atmospheres. 2011 Mar 16;116(D5).

29. Sahraei J, Mobarak Hassan E, Mohammadi N. The Effect of the Zagros Mountain Range on Transporting Iraqi Dust to Western Iran using the WRF/Chem Model (Case Study). Journal of Geography and Environmental Hazards. 2020 Jan 21;8(4):119-34.

30. Marticorena B, Bergametti G. Modeling the atmospheric dust cycle: 1. Design of a soil-derived dust emission scheme. Journal of geophysical research: atmospheres. 1995 Aug 20;100(D8):16415-30.

31. Mlawer EJ, Taubman SJ, Brown PD, Iacono MJ, Clough SA. Radiative transfer for inhomogeneous atmospheres: RRTM, a validated correlated-k model for the longwave. Journal of Geophysical Research: Atmospheres. 1997. Jul 27; 102(D14):16663-82.

32. Chou MD, Suarez MJ. A solar radiation parameterization for atmospheric studies. 1999. Jun 1.

33. Chen F, Dudhia J. Coupling an advanced land surface–hydrology model with the Penn State–NCAR MM5 modeling system. Part I: Model implementation and sensitivity. Monthly weather review. 2001 Apr 1; 129(4):569-85.

34. Noh Y, Cheon WG, Hong SY, Raasch S. Improvement of the K-profile model for the planetary boundary layer based on large eddy simulation data. Boundary-layer meteorology. 2003 May; 107(2):401-27.

35. Hong SY, Noh Y, Dudhia J. A new vertical diffusion package with an explicit treatment of entrainment processes. Monthly weather review. 2006 Sep 1;134(9):2318-41.

36. Grell GA. Prognostic evaluation of assumptions used by cumulus parameterizations. Monthly weather review. 1993 Mar;121(3):764-87.

37. Fuell KK, Guyer BJ, Kann D, Molthan AL, Elmer N. Next Generation Satellite RGB Dust Imagery Leads to Operational Changes at NWS Albuquerque. Journal of Operational Meteorology. 2016 Mar 15;4(6).

38. Fuell, K. and Guyer, B., 2014, February. Integration of RGB" Dust" Imagery to Operations at the Albuqueque Forecast Office. In American Meteorological Socie! y (AMS) Annual Meeting (No. M14-3302).

39. Beegum SN, Gherboudj I, Chaouch N, Temimi M, Ghedira H. Simulation and analysis of synoptic scale dust storms over the Arabian Peninsula. Atmospheric Research. 2018 Jan 1;199:62-81.

40. Hamzeh NH (a), Karami S, Opp C, Fattahi E, Jean-François V. Spatial and temporal variability in dust storms in the Middle East, 2002–2018: three case studies in July 2009. Arabian Journal of Geosciences. 2021 Apr;14(7):1-4.

41. Mostafaeipour A, Abarghooei H. Harnessing wind energy at Manjil area located in north of Iran. Renewable and Sustainable Energy Reviews. 2008 Aug 1;12(6):1758-66.

42. Hamzeh NH, Karami S, Kaskaoutis DG, Tegen I, Moradi M, Opp C. Atmospheric dynamics and numerical simulations of six frontal dust storms in the Middle East region. Atmosphere. 2021 Jan 18;12(1):125.